iScience, Volume *23*

Supplemental Information

MR1-Restricted T Cells with MAIT-like Characteristics Are Functionally Conserved in the Pteropid Bat *Pteropus alecto*

Edwin Leeansyah, Ying Ying Hey, Wan Rong Sia, Justin Han Jia Ng, Muhammad Yaaseen Gulam, Caroline Boulouis, Feng Zhu, Matae Ahn, Jeffrey Y.W. Mak, David P. Fairlie, Andrea Lay Hoon Kwa, Johan K. Sandberg, and Lin-Fa Wang

Supplementary Materials

A

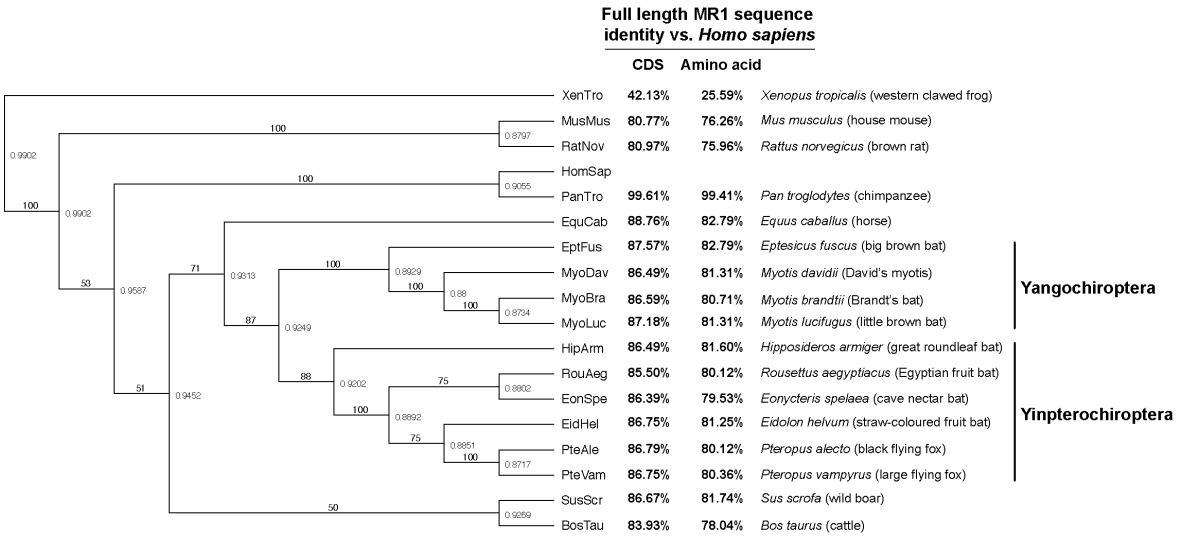

B

	HomSap	PanTro	MusMus	RatNov	EquCab	BosTau	SusScr	EptFus	MyoDav	MyoBra	MyoLuc	HipArm	RouAeg	EonSpe	EidHel	PteAle	PteVam	XenTro
HomSap		99.61%	80.77%	80.97%	88.76%	83.93%	86.67%	87.57%	86.49%	86.59%	87.18%	86.49%	85.50%	86.39%	86.75%	86.79%	86.75%	42.13%
PanTro	99.61%		80.77%	81.16%	88.95%	84.22%	86.87%	87.77%	86.69%	86.79%	87.38%	86.69%	85.60%	86.49%	86.84%	86.88%	86.84%	42.33%
MusMus	80.77%	80.77%		90.12%	79.29%	75.94%	78.11%	78.01%	78.80%	78.01%	78.40%	77.91%	75.54%	76.04%	76.95%	77.51%	77.35%	40.25%
RatNov	80.97%	81.16%	90.12%		79.98%	76.82%	77.91%	79.09%	79.19%	79.09%	79.09%	78.60%	77.22%	77.81%	78.54%	78.90%	78.73%	40.63%
EquCab	88.76%	88.95%	79.29%	79.98%		84.91%	87.26%	88.07%	87.77%	87.67%	88.26%	87.48%	87.18%	87.97%	88.33%	88.56%	88.53%	41.15%
BosTau	83.93%	84.22%	75.94%	76.82%	84.91%		86.67%	85.11%	85.11%	84.71%	85.01%	84.12%	84.02%	84.91%	84.77%	84.91%	84.77%	42.03%
SusScr	86.67%	86.87%	78.11%	77.91%	87.26%	86.67%		86.67%	86.27%	85.87%	86.27%	84.98%	85.07%	85.97%	86.07%	86.77%	86.47%	41.54%
EptFus	87.57%	87.77%	78.01%	79.09%	88.07%	85.11%	86.67%		95.17%	95.07%	95.66%	87.48%	86.88%	88.26%	88.13%	88.66%	88.82%	41.25%
MyoDav	86.49%	86.69%	78.80%	79.19%	87.77%	85.11%	86.27%	95.17%		97.14%	97.73%	88.26%	87.18%	87.77%	88.03%	88.36%	88.33%	40.76%
MyoBra	86.59%	86.79%	78.01%	79.09%	87.67%	84.71%	85.87%	95.07%	97.14%		98.82%	88.07%	86.69%	87.67%	87.73%	88.07%	88.03%	41.06%
MyoLuc	87.18%	87.38%	78.40%	79.09%	88.26%	85.01%	86.27%	95.66%	97.73%	98.82%		88.46%	87.18%	88.26%	88.23%	88.66%	88.63%	41.15%
HipArm	86.49%	86.69%	77.91%	78.60%	87.48%	84.12%	84.98%	87.48%	88.26%	88.07%	88.46%		87.18%	88.56%	88.72%	89.15%	88.92%	39.98%
RouAeg	85.50%	85.60%	75.54%	77.22%	87.18%	84.02%	85.07%	86.88%	87.18%	86.69%	87.18%	87.18%		95.36%	93.47%	93.98%	93.97%	41.25%
EonSpe	86.39%	86.49%	76.04%	77.81%	87.97%	84.91%	85.97%	88.26%	87.77%	87.67%	88.26%	88.56%	95.36%		95.85%	96.55%	96.34%	41.15%
EidHel	86.75%	86.84%	76.95%	78.54%	88.33%	84.77%	86.07%	88.13%	88.03%	87.73%	88.23%	88.72%	93.47%	95.85%		96.54%	96.34%	40.98%
PteAle	86.79%	86.88%	77.51%	78.90%	88.56%	84.91%	86.77%	88.66%	88.36%	88.07%	88.66%	89.15%	93.98%	96.55%	96.54%		99.21%	40.57%
PteVam	86.75%	86.84%	77.35%	78.78%	88.53%	84.77%	86.47%	88.82%	88.33%	88.03%	88.63%	88.92%	93.97%	96.34%	96.34%	99.21%		40.59%
XenTro	42.13%	42.33%	40.25%	40.63%	41.15%	42.03%	41.54%	41.25%	40.76%	41.06%	41.15%	39.98%	41.25%	41.15%	40.98%	40.57%	40.59%	

C

	HomSap	PanTro	MusMus	RatNov	EquCab	BosTau	SusScr	EptFus	MyoDav	MyoBra	MyoLuc	HipArm	RouAeg	EonSpe	EidHel	PteAle	PteVam	XenTro
HomSap		99.41%	76.26%	75.96%	82.79%	78.04%	81.74%	82.79%	81.31%	80.71%	81.31%	81.60%	80.12%	79.53%	81.25%	80.12%	80.36%	25.59%
PanTro	99.41%		76.85%	76.26%	83.38%	78.64%	82.34%	83.38%	81.90%	81.31%	81.90%	82.20%	80.42%	79.82%	81.55%	80.42%	80.65%	25.88%
MusMus	76.26%	76.85%		88.05%	73.59%	70.92%	74.78%	76.26%	76.56%	75.37%	76.26%	76.26%	72.70%	71.81%	74.70%	73.89%	73.51%	23.70%
RatNov	75.96%	76.26%	88.05%		74.48%	72.40%	73.59%	76.85%	75.96%	76.56%	76.56%	76.26%	74.48%	74.18%	75.89%	74.78%	74.40%	24.86%
EquCab	82.79%	83.38%	73.59%	74.48%		78.04%	80.84%	82.79%	81.90%	80.42%	81.31%	81.31%	79.53%	80.12%	82.44%	80.71%	81.25%	26.47%
BosTau	78.04%	78.64%	70.92%	72.40%	78.04%		79.04%	80.12%	79.53%	78.34%	78.64%	77.74%	77.74%	77.74%	77.68%	75.37%	75.89%	26.47%
SusScr	81.74%	82.34%	74.78%	73.59%	80.84%	79.04%		81.74%	80.54%	79.94%	80.24%	79.94%	79.04%	79.04%	80.54%	79.94%	79.34%	24.12%
EptFus	82.79%	83.38%	76.26%	76.85%	82.79%	80.12%	81.74%		93.77%	93.47%	94.36%	84.57%	83.09%	82.79%	84.23%	82.79%	83.33%	25.59%
MyoDav	81.31%	81.90%	76.56%	75.96%	81.90%	79.53%	80.54%	93.77%		95.55%	96.44%	85.46%	83.38%	82.79%	83.93%	82.20%	82.74%	26.47%
MyoBra	80.71%	81.31%	75.37%	76.56%	80.42%	78.34%	79.94%	93.47%	95.55%		97.92%	84.87%	81.60%	81.31%	82.14%	80.12%	80.65%	26.18%
MyoLuc	81.31%	81.90%	76.26%	76.56%	81.31%	78.64%	80.24%	94.36%	96.44%	97.92%		84.87%	82.49%	82.49%	83.04%	81.31%	81.85%	26.18%
HipArm	81.60%	82.20%	76.26%	76.26%	81.31%	77.74%	79.94%	84.57%	85.46%	84.87%	84.87%		81.60%	81.31%	81.85%	81.60%	81.55%	25.29%
RouAeg	80.12%	80.42%	72.70%	74.48%	79.53%	77.74%	79.04%	83.09%	83.38%	81.60%	82.49%	81.60%		93.47%	90.77%	90.21%	90.48%	25.88%
EonSpe	79.53%	79.82%	71.81%	74.18%	80.12%	77.74%	79.04%	82.79%	82.79%	81.31%	82.49%	81.31%	93.47%		92.56%	92.28%	92.86%	26.47%
EidHel	81.25%	81.55%	74.70%	75.89%	82.44%	77.68%	80.54%	84.23%	83.93%	82.14%	83.04%	81.85%	90.77%	92.56%		93.75%	94.35%	25.96%
PteAle	80.12%	80.42%	73.89%	74.78%	80.71%	75.37%	79.94%	82.79%	82.20%	80.12%	81.31%	81.60%	90.21%	92.28%	93.75%		98.81%	25.29%
PteVam	80.36%	80.65%	73.51%	74.40%	81.25%	75.89%	79.34%	83.33%	82.74%	80.65%	81.85%	81.55%	90.48%	92.86%	94.35%	98.81%		24.78%
XenTro	25.59%	25.88%	23.70%	24.86%	26.47%	26.47%	24.12%	25.59%	26.47%	26.18%	26.18%	25.29%	25.88%	26.47%	25.96%	25.29%	24.78%	

Figure S1. Comparison of MR1 sequence identities between various bats species and selected placental mammals. Related to Figure 1. (A) Phylogenetic tree of MR1 sequence identity and a summary of full length MR1 sequence identity of indicated animals with that of humans. **(B, C)** Comparison of full length MR1 nucleotide **(B)** and translated amino acid **(C)** sequence identity of indicated animals, with particular emphasis on human, mouse, and *P. alecto* sequences (coloured boxes).

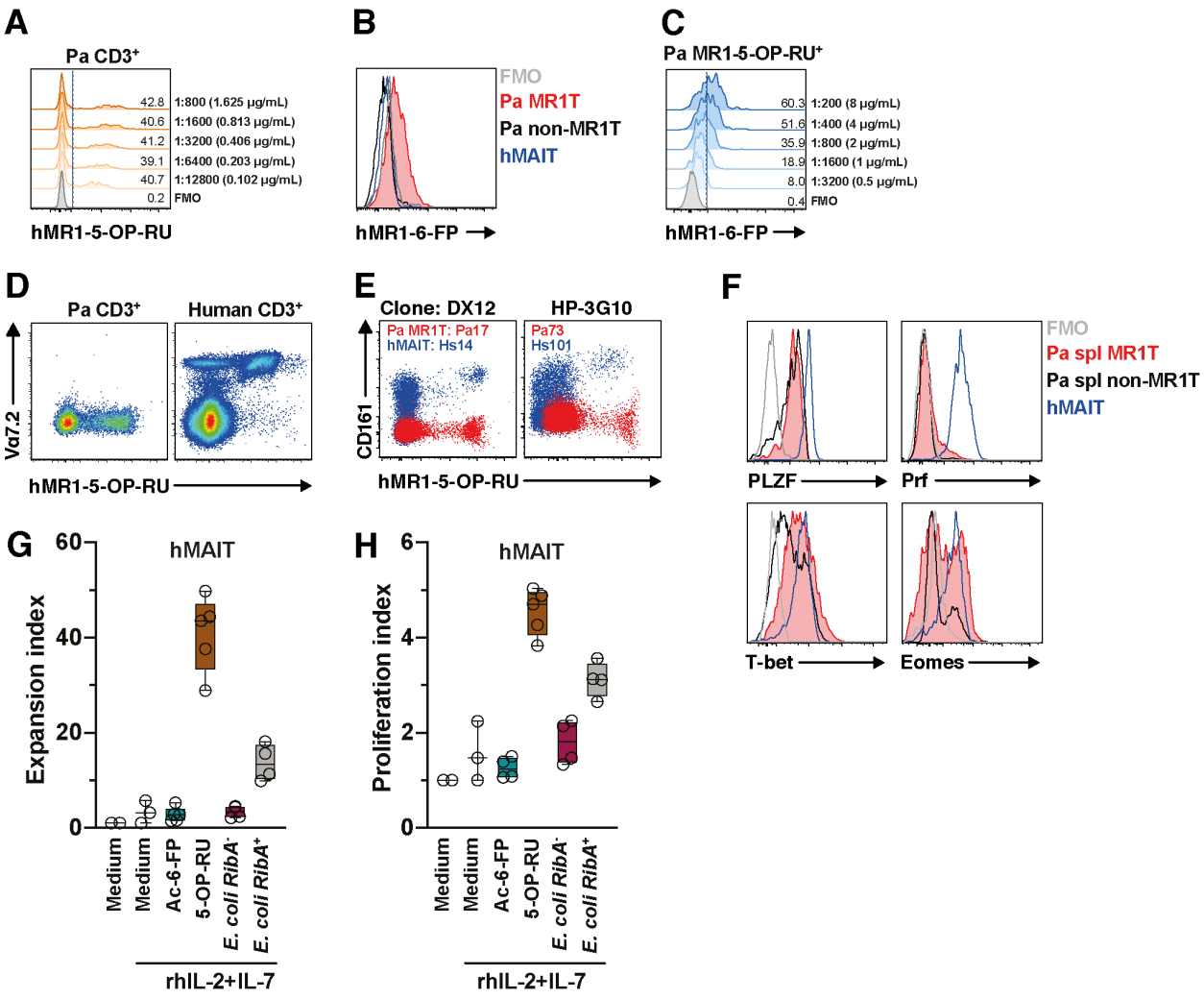

Figure S2. Characteristics of MR1T cells in *P. alecto* bats. Related to Figures 1 and 2. (A) A representative histogram of the titration of the hMR1-5-OP-RU tetramer on freshly thawed Pa BM MNC (n=3). **(B)** Binding and **(C)** titration of hMR1-6-FP tetramer to Pa MR1T, Pa non-MR1T, or hMAIT cells as indicated (n=3). **(D)** Staining of V**α**7.2 TCR using mAb clone 3C10 and **(E)** CD161 using mAb clones DX12 and HP-3G10 on Pa BM MNC and hPBMC (n>5). **(F)** Expression of the transcription factors PLZF, T-bet, and Eomes, and the cytolytic protein Prf on spleen Pa MR1T, Pa non-MR1T, and PB hMAIT cells (n>5). **(G)** Expansion and **(H)** proliferation indices of hMAIT cells following stimulation with various antigens as indicated (n=2-4). Box and whisker plot shows all data points, median, and the interquartile range.

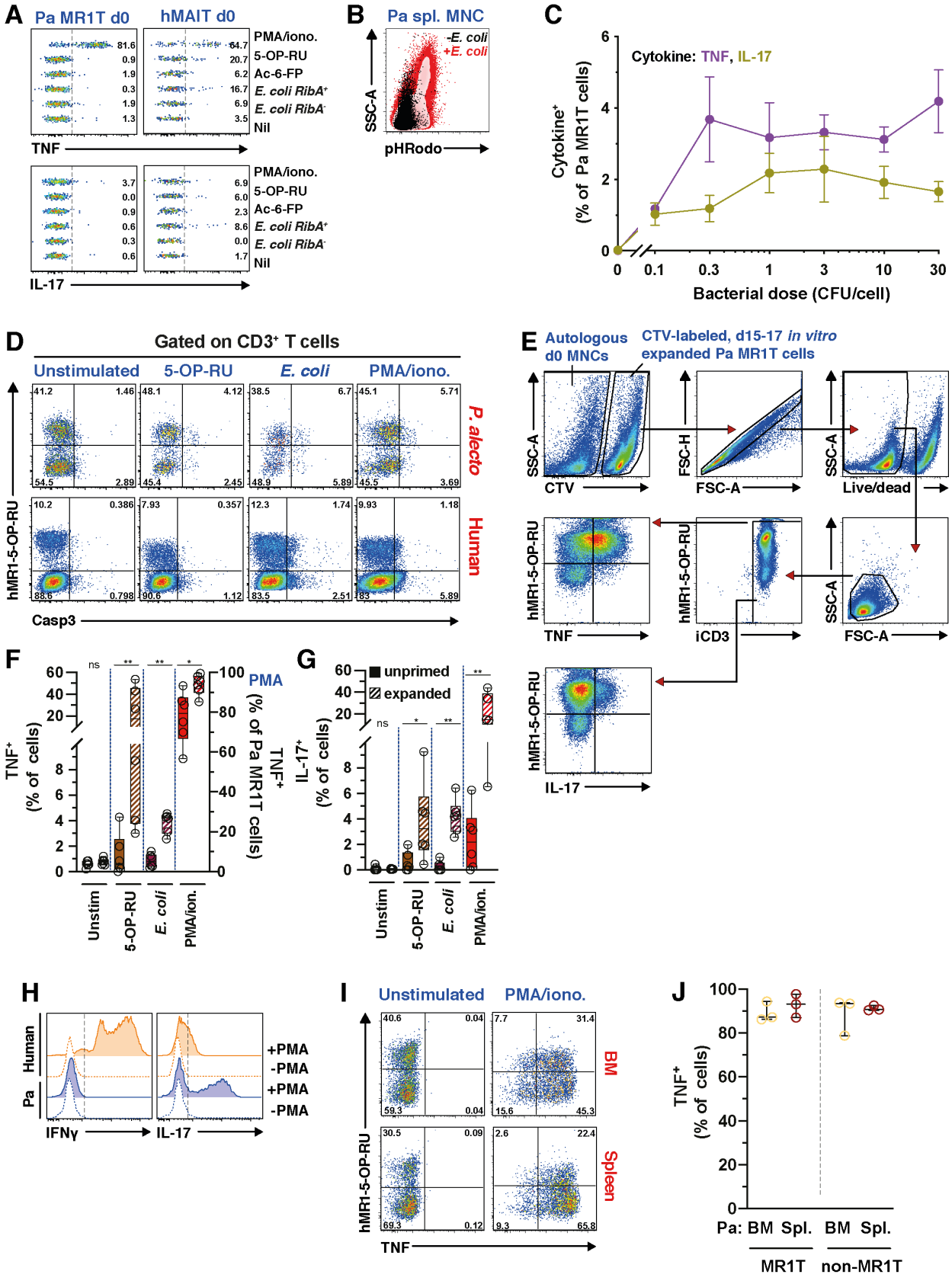
A
Pa MR1T d0
hMAIT d0
PMA/iono.
5-OP-RU
Ac-6-FP
E. coli RibA+
E. coli RibA-
Nil
TNF
IL-17
B
Pa spl. MNC
-E. coli
+E. coli
SSC-A
pHRodo
C
Cytokine: TNF, IL-17
Cytokine+ (% of Pa MR1T cells)
Bacterial dose (CFU/cell)
D
Gated on CD3+ T cells
Unstimulated
5-OP-RU
E. coli
PMA/iono.
P. alecto
Human
hMR1-5-OP-RU
Casp3
E
Autologous d0 MNCs
CTV-labeled, d15-17 in vitro expanded Pa MR1T cells
SSC-A
CTV
FSC-H
FSC-A
Live/dead
TNF
iCD3
IL-17
F
TNF+ (% of cells)
PMA
TNF+ (% of Pa MR1T cells)
Unstim
5-OP-RU
E. coli
PMA/ion.
G
unprimed
expanded
IL-17+ (% of cells)
H
Human
Pa
+PMA
-PMA
IFNγ
IL-17
I
Unstimulated
PMA/iono.
BM
Spleen
hMR1-5-OP-RU
TNF
J
TNF+ (% of cells)
Pa: BM Spl. BM Spl.
MR1T
non-MR1T

Figure S3. Pa MR1T cells expression of pro-inflammatory cytokine following various stimulations. Related to Figures 4 and 5. (A) Expression of TNF and IL-17 by resting BM Pa MR1T and PB hMAIT cells following 8 h stimulations with various antigens (n=7). **(B)** Uptake of *E. coli* EC120S by freshly-thawed Pa spleen MR1T cells as assessed by pHRodo fluorescence (n=2). **(C)** TNF and IL-17 production by freshly-thawed Pa BM MR1T cells following 24 h incubation with formaldehyde-fixed *E. coli* EC120S at various bacterial dose (3 independent repeats of the same donor Pa bat). **(D)** Representative FACS plots of active Caspase 3 expression by freshly-thawed Pa BM MR1T cells and hMAIT cells following 24 h culture with MR1 ligand 5-OP-RU or E. coli EC120S, or 6 h with PMA/ionomycin (n=3-6). **(E)** Gating and experimental strategy of expanded (d15-17) Pa MNC co-culture with freshly-thawed autologous Pa MNC to determine the expression of TNF and IL-17 by expanded Pa MR1T and non-MR1T cells. **(F, G)** Comparison of **(F)** TNF and **(G)** IL-17 production by unprimed and expanded Pa BM MR1T cells following 24 h culture with MR1 ligand 5-OP-RU or E. coli EC120S, or 6 h culture with PMA/ionomycin (n=6). **(H)** Detection of IFN**γ** using IL-17 as an experimental positive control in Pa CD3+ and hCD3+ T cells following 6 h of PMA/ionomycin stimulation. **(I, J)** Expression of TNF by expanded BM and spleen Pa MR1T and non-MR1T cells after 8 h stimulation with PMA/ionomycin (n=3). Box and whisker plot shows all data points, median, and the interquartile range. Error bars on the line graph depict standard error. Statistical significance was determined using the Mann-Whitney test **(F, G)**. ** $p<0.01$,* $p<0.05$. ns, not significant.

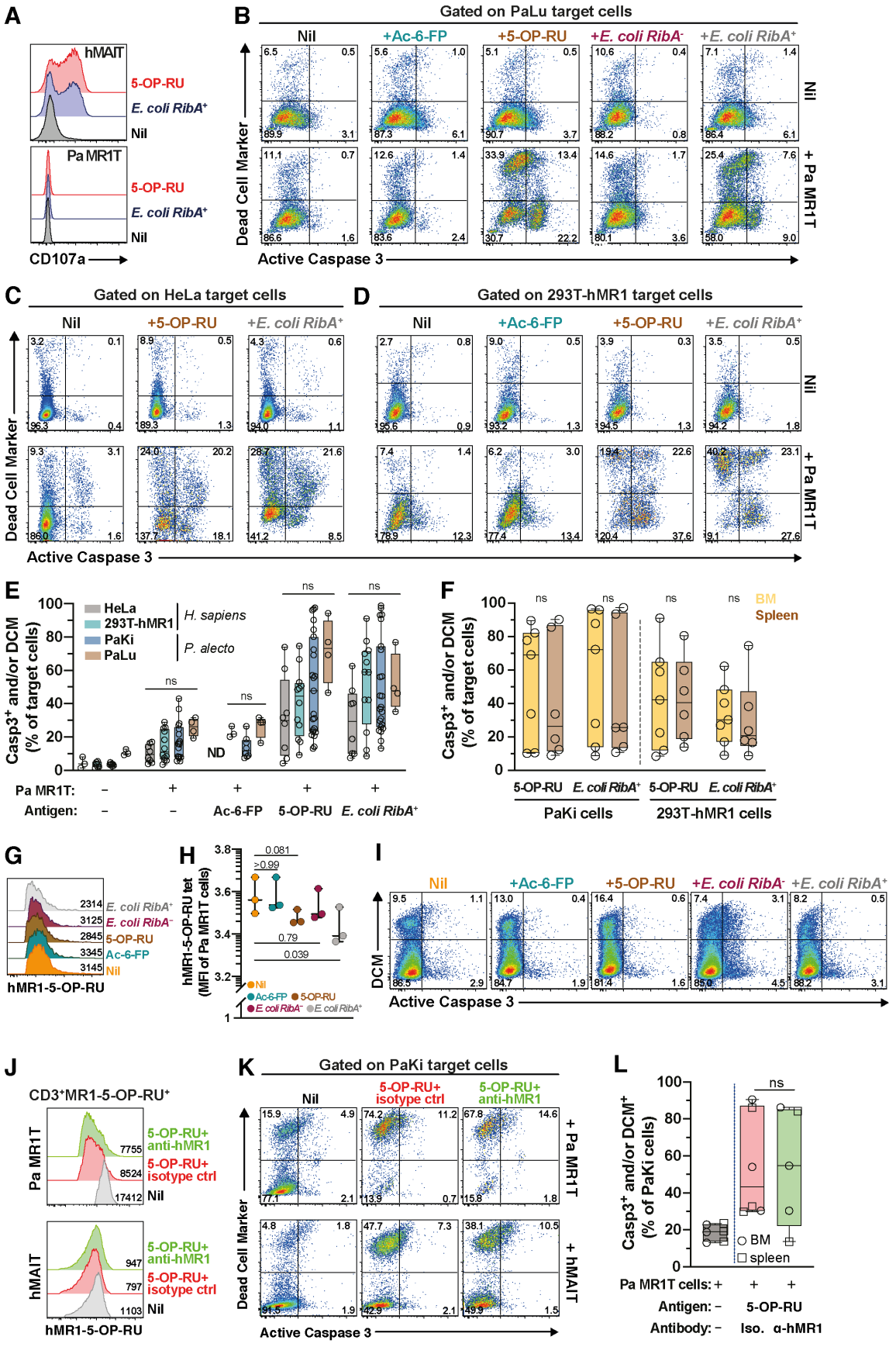
A
hMAIT
5-OP-RU
E. coli RibA+
Nil
Pa MR1T
5-OP-RU
E. coli RibA+
Nil
CD107a
B
Gated on PaLu target cells
Nil
+Ac-6-FP
+5-OP-RU
+E. coli RibA-
+E. coli RibA+
Dead Cell Marker
Active Caspase 3
Nil
+ Pa MR1T
C
Gated on HeLa target cells
Nil
+5-OP-RU
+E. coli RibA+
D
Gated on 293T-hMR1 target cells
Nil
+Ac-6-FP
+5-OP-RU
+E. coli RibA+
E
Casp3+ and/or DCM (% of target cells)
HeLa
293T-hMR1
PaKi
PaLu
H. sapiens
P. alecto
ns
ND
Pa MR1T:
Antigen:
Ac-6-FP
5-OP-RU
E. coli RibA+
F
Casp3+ and/or DCM (% of target cells)
ns
BM
Spleen
5-OP-RU
E. coli RibA+
PaKi cells
293T-hMR1 cells
G
2314 E. coli RibA+
3125 E. coli RibA-
2845 5-OP-RU
3345 Ac-6-FP
3145 Nil
hMR1-5-OP-RU
H
hMR1-5-OP-RU tet (MFI of Pa MR1T cells)
0.081
>0.99
0.79
0.039
Nil
Ac-6-FP
5-OP-RU
E. coli RibA-
E. coli RibA+
I
Nil
+Ac-6-FP
+5-OP-RU
+E. coli RibA-
+E. coli RibA+
DCM
Active Caspase 3
J
CD3+MR1-5-OP-RU+
Pa MR1T
7755 5-OP-RU+ anti-hMR1
8524 5-OP-RU+ isotype ctrl
17412 Nil
hMAIT
947 5-OP-RU+ anti-hMR1
797 5-OP-RU+ isotype ctrl
1103 Nil
hMR1-5-OP-RU
K
Gated on PaKi target cells
Nil
5-OP-RU+ isotype ctrl
5-OP-RU+ anti-hMR1
Dead Cell Marker
Active Caspase 3
+ Pa MR1T
+ hMAIT
L
Casp3+ and/or DCM+ (% of PaKi cells)
ns
BM
spleen
Pa MR1T cells: +
Antigen: -
5-OP-RU
Antibody: -
Iso.
α-hMR1

Figure S4. MR1-dependence and -cross-reactivity of Pa MR1T cell cytotoxic effector function. Related to Figure 6. (A) Detection of the degranulation marker (CD107a) by Pa MR1T and hMAIT cells following 24 h co-culture with 5-OP-RU-pulsed Pa kidney (PaKi) cell line (n>5). **(B, C, D, E)** Flow cytometry plots and expression of active caspase (Casp)3 and amine-reactive cytoplasmic dye (dead cell marker; DCM) by the Pa lung (PaLu), human HeLa, and 293T cells stably transfected with hMR1 (293T-hMR1) target cells fed with various antigens as indicated following 24 h co-culture with expanded (d15-17) Pa MR1T cells (n=3-23). **(F)** Comparison of killing ability of BM and spleen Pa MR1T cells against PaKi cells and 293T-hMR1 cells (% Casp3+ and/or DCM+) pre-pulsed with 5-OP-RU or *E. coli RibA*$^{+}$ EC120S (n=6-7). **(G)** Histograms and **(H)** levels (MFI) of the MR1-5-OP-RU tetramer staining of resting Pa MR1T cells and **(I)** PaKi cell line apoptosis following 24 h co-culture under various stimulations as indicated (n=3). **(J, K, L)** Histograms and MFI of the MR1-5-OP-RU tetramer staining of expanded Pa MR1T cells or hMAIT cells **(J)** and 5-OP-RU-pulsed PaKi target cells apoptosis **(K, L)** following 24 h co-culture, in the presence of anti-hMR1 mAb or IgG2a isotype control (n=5-6). Box and whisker plot shows all data points, median, and the interquartile range. Statistical significance was determined using mixed-effects analysis **(E)**, Wilcoxon's signed-rank test **(F)**, the Friedman test with Dunn's multiple comparison test **(H)**, and the Mann-Whitney test **(L)**. ns, not significant.

Table S1. Flow cytometry-based antibodies and reagents used in the study. Related to Figures 1-6.

Reagent Name	Clone	Source
Anti-human RORγt BV650	Q21-559	BD Biosciences
Anti-human active Caspase 3 BV650	C92-605	
Anti-human CD107a – BUV395	H4A3	
Anti-human/mouse CD11b BV711	M1/70	Biolegend
Anti-mouse Ly6C PE-Cy7	HK1.4	
Anti-human TNF BV711	MAb11	
Anti-human IL17A BV786	BL168	
Anti-human CD3ε-FITC	CD3-12	Bio-Rad
Anti-human/mouse CD44 APC-e780	IM7	ThermoFisher
Anti-human Eomes PE-610	WD1928	
Anti-human T-bet PE-Cy7	eBio4BIO	
pHRodo Red, succinimidyl ester	Not applicable	
LIVE/DEAD® Fixable Near-IR Dead Cell Stain Kits	Not applicable	Invitrogen
CellTrace™ Violet Cell Proliferation Kit	Not applicable	
Anti-human Perforin PF647	Pf-344	Mabtech
Anti-human IL-17A FITC	MTF504	
Anti-ferret IFNγ PF647P	MTF14	
Anti-human PLZF APC	R17-809	R&D
Human MR1-5-OP-RU tetramer PE	Not applicable	The NIH tetramer Core Facility Emory University
Human MR1-6-FP tetramer BV421, AF680	Not applicable	

Text S1. Extended acknowledgement list for Duke-NUS bat processing team: Justin Han Jia Ng, Yok Teng Chionh, Wan Ni Chia, Geraldine Goh, Kong Pui San, Aaron T. Irving, Anna Uehara, Ying Ying Hey, Pritisha Rozario, Randy Foo, Wan Shoo Cheong, Pravin Periasamy, the Queensland Animal Science Precinct team led by Milou Dekkers, Hume Fields, Vicky Boyd, Gary Crameri, Prof. Joanne Meers and staff at the School of Veterinary Science, University of Queensland, Trish Wimberley and staff at the Australian Bat Clinic & Wildlife Trauma Centre, Bat Conservation & Rescue Queensland.

Transparent Methods

P. alecto tissue and human blood processing

All procedures in this study dealing with animal samples complied with all relevant ethical regulations. Specifically, capturing and processing of Pa in Australia was approved by the Queensland Animal Science Precinct and University of Queensland Animal Ethics Committee (AEC#SVS/073/16/USGMS) and the Australian Animal Health Laboratory (AAHL) Animal Ethics Committee (AEC#1389 and AEC#1557). Where possible, wild bats with irreparable physical damage (torn wings) already scheduled for euthanasia were utilized. Processing of bat peripheral blood, bone marrow (BM), and spleen, as described previously (Ahn et al., 2019; Ahn et al., 2016; Gamage et al., 2020; Martinez Gomez et al., 2016), were shipped to Duke-NUS Medical School, Singapore. Human samples were collected after informed written consent was obtained from all donors in accordance with study protocols conforming to the provisions of the Declaration of Helsinki. Ethics approval was obtained from the National University of Singapore Institutional Review Board (NUS-IRB reference codes B-15-088 and H-18-029). Human peripheral blood was collected from healthy donors recruited at the apheresis unit, Bloodbank@HSA, Health Services Authority, Singapore. Peripheral blood mononuclear cells (PBMCs) were isolated by standard Ficoll-Histopaque density gradient separation (Ficoll-Histopaque Premium; GE Healthcare). After isolation, all samples were cryo-preserved in 90% fetal bovine serum (FBS) and 10% DMSO in liquid nitrogen until further use.

Bacterial culture and preparation

The *E. coli* laboratory strain *RibA*$^{+}$, riboflavin-synthesis competent 1100-2 and its *RibA*-deficient, riboflavin-synthesis incompetent congenic strain BSV18 were obtained from the Coli Genetic Stock Center, Yale University. The riboflavin-synthesis competent, clinical strain EC120S was isolated from a patient suffering from a blood infection and retrieved from the Singapore General Hospital archived bacteria repository (Boulouis et al., 2020; Lim et al., 2018). For Pa MR1T and human MAIT cell stimulation assays, all *E. coli* strains were grown overnight at 37 °C in Luria (lysogeny) broth (LB) with shaking, enumerated, and frozen in -80 °C until further use as described (Dias et al., 2017; Sia et al., 2020). *RibA*$^{-}$ BSV18 cultures were supplemented with 20 µg/mL riboflavin (Sigma-Aldrich) (Dias et al., 2018).

Preparation of MAIT cell antigen 5-OP-RU

The MAIT cell antigen 5-(2-oxopropylideneamino)-6-D-ribitylaminouracil (5-OP-RU) was synthesised according to a previously optimised procedure (Mak et al., 2017). It is stable in DMSO, but exposure time to aqueous media should be minimised as much as possible to maximise activity, as 5-OP-RU converts rapidly to a much less active lumazine in water (Mak et al., 2017).

Assessment of *E. coli* internalisation

To determine *E. coli* internalisation by Pa MNC, *E. coli* strain EC120S were labelled with pHRodo Red (Thermo Fisher Scientific Life Sciences) as previously described (Dias et al., 2016). Labelled *E. coli* were then fed to Pa MNC for 3 h at 37 °C.

Identification of MR1T cell population and flow cytometry analysis

Cell surface and intracellular staining for cytokines, cytotoxic molecules, transcription factors, and active caspase 3 was performed as previously described (Dias et al., 2018; Dias et al., 2017). Staining with the hMR1-5-OP-RU-PE and hMR1-6-FP-BV421 tetramers was performed concurrently for 40 min at room temperature (RT) (Corbett et al., 2014) before proceeding to the surface and intracellular staining with other mAbs (Table S1.) In selected experiments, Pa MNCs were first incubated with titrated concentrations of hMR1-5-OP-RU-PE or hMR1-6-FP-BV421 tetramer, followed by incubation with a fixed optimal

concentration of hMR1-6-FP-BV421 or hMR1-5-OP-RU-PE tetramer, respectively. $CD3^+$ T cells were identified by intracellular staining with the CD3–12 mAb (Table S1) as previously described (Gamage et al., 2020; Martinez Gomez et al., 2016), which detects a highly conserved epitope on the cytoplasmic domain of CD3**ε** (Martinez Gomez et al., 2016). Samples were acquired on an LSRFortessa flow cytometer (BD Biosciences) equipped with 355, 405, 488, 561, and 640 nm lasers. Single-stained polystyrene beads (BD Biosciences) and the compensation platform in FACSDiva v. 8.0.1 (BD Biosciences) or FlowJo software v. 9.9 (TreeStar) were used for compensation.

P. alecto MR1T cell and human MAIT cell expansion and proliferation assay

Our previously described MAIT cell expansion and proliferation assessment methodologies for hMAIT cells (Boulouis et al., 2020; Sia et al., 2020) were adapted for the current study. Briefly, cryopreserved MNC of Pa BM, spleen, as well as human peripheral blood were thawed and cultured at $5x10^6$ cells/mL in ImmunoCult-XF T cell expansion medium (Stemcell Technologies) supplemented with 8% CTS Immune cell serum replacement (Invitrogen), 5 ng/mL recombinant human(rh) IL-2 (Peprotech), 10 ng/mL rhIL-7 (R&D), 50 µg/mL gentamicin (Gibco), and 100 µg/mL Normocin (Invivogen) (complete expansion medium). Cells were stimulated with 10 nM 5-OP-RU on day 0, 5, and 10, and the culture media was changed every 2-3 days. On day 11, viable cells were isolated by Ficoll-Histopaque density gradient centrifugation. Cells were harvested for functional assay on day 15-17.

To assess Pa MR1T cell proliferation, cryopreserved Pa BM MNC and human PBMC were thawed and stained with 1.25 µM CellTrace Violet (CTV; Thermo Fisher Scientific Life Sciences). Cells were then stimulated with various synthetic and microbial antigens in complete expansion medium, including the MR1 ligands 5-OP-RU (10 nM) or acetyl-6-formyl pterin (Ac-6-FP; 25 µM) (Shircks Laboratories), or formaldehyde-fixed *E. coli* at a bacterial dose of 0.1 colony-forming units (CFU)/cell, using strains 1100-2 or BSV18. Expansion and proliferation indices of Pa MR1T cells (defined as hMR1-5-OP-RU^+ $CD3^+$ lymphocytes) and hMAIT cells (defined as were then determined based on CTV dilution at day 5 post-stimulation using the FlowJo v 9.9 software (Tree Star Inc). In selected experiments, cultures were continued up to day 10 post-stimulation to determine expression of Prf and various transcription factors.

P. alecto MR1T cell cytokine assay

Freshly thawed and rested Pa BM MNC and human PBMCs (d0) cells were stimulated for 2 h with the MR1 ligand 5-OP-RU (2 nM) or Ac-6-FP (25 µM), or 3 h with formaldehyde-fixed *E. coli* (Dias et al., 2016) strains EC120S, 1100-2, or BSV18 (bacterial dose: 3 CFU/cell). These cells, serving as antigen-presenting cells, were then co-cultured for 6-72 h as indicated with CTV-labelled autologous Pa MR1T cells or hMAIT cells that had been expanded for 15-17 days. Monensin was added to all wells and cells in the last 6 h of culture. PMA/ionomycin stimulation (BD Leukocyte Activator, BD Biosciences) was included as positive control. In selected experiments, the freshly thawed d0 cells were directly assessed for cytokine production without addition of expanded Pa MR1T cells or hMAIT cells.

P. alecto MR1T cell cytotoxicity assay

Immortalised *P. alecto* kidney cells (PaKi) and *P. alecto* lung cells (PaLu) were cultured in high glucose DMEM medium (Gibco) supplemented with 10% fetal bovine serum (FBS) (Gibco or Hyclone). Human 293T cells stably transfected with human MR1 (293T-hMR1) and HeLa cells were maintained in RPMI medium (Gibco) supplemented with 10% FBS, 50 µg/mL gentamicin, and 100 µg/mL normocin. Pa MR1T cell cytotoxicity assay was adapted from our previously described protocols (Dias et al., 2016; Sia et al., 2019). Briefly, PaKi, PaLu, HeLa, and 293T-hMR1 target cell lines were pulsed with 2 nM 5-OP-RU, 25 µM Ac-6-FP, or 30 colony-forming units (CFU)/cell *E. coli* strains EC120S, 1100-2, or BSV18 for 3 h. Pa MR1T cells that have been expanded for 15-17 days were labelled with 1 µM CTV and co-cultured with pulsed target

cells at an effector to target cell (E:T) ratio of 10:1. After 24 h of co-culture, cells were trypsinised and stained to detect target cell death using anti-active caspase 3 mAb (BD Biosciences) coupled with amine-reactive live/dead cell marker (DCM) (Invitrogen). In selected experiments, expanded human MAIT cell killing of pulsed target cells were included as controls.

MR1 sequence comparison

All MR1 CoDing Sequences (CDS) were retrieved by MegaBLAST of human MR1 genomic sequence against bat genomes and then translated into amino acid sequences. Comparisons of the human MR1 CDS and amino acid sequence were also made with those of other selected placental mammals and amphibians as indicated. A neighbour-joining tree with bootstrap number of 100 was plotted by the translation alignment of all MR1 CDS.

Statistical analysis

Statistical analyses were performed using Prism software v.8.3.0 (GraphPad). Data sets were first assessed for data normality distribution using the Shapiro-Wilk normality test. Statistically significant differences between samples were determined using the unpaired t-test for parametric data, or Mann-Whitney's test for unpaired non-parametric data, and the paired t-test for parametric matched data, or Wilcoxon's signed-rank test for non-parametric matched data. The Kruskal-Wallis ANOVA, the Friedman test, or mixed-effects analysis followed by Dunn's multiple comparison post-hoc test as indicated was used to detect differences across multiple samples. Correlations were assessed using the Spearman correlation. Two-sided p-values < 0.05 were considered significant.

References

Ahn, M., Anderson, D.E., Zhang, Q., Tan, C.W., Lim, B.L., Luko, K., Wen, M., Chia, W.N., Mani, S., Wang, L.C., *et al.* (2019). Dampened NLRP3-mediated inflammation in bats and implications for a special viral reservoir host. Nat. Microbiol. *4*, 789-799.

Ahn, M., Cui, J., Irving, A.T., and Wang, L.F. (2016). Unique Loss of the PYHIN Gene Family in Bats Amongst Mammals: Implications for Inflammasome Sensing. Sci. Rep. *6*, 21722.

Boulouis, C., Sia, W.R., Gulam, M.Y., Teo, J.Q.M., Png, Y.T., Phan, T.K., Mak, J.Y.W., Fairlie, D.P., Poon, I.K.H., Koh, T.H., *et al.* (2020). Human MAIT cell cytolytic effector proteins synergize to overcome carbapenem resistance in Escherichia coli. PLoS Biol. *18*, e3000644.

Corbett, A.J., Eckle, S.B., Birkinshaw, R.W., Liu, L., Patel, O., Mahony, J., Chen, Z., Reantragoon, R., Meehan, B., Cao, H., *et al.* (2014). T-cell activation by transitory neo-antigens derived from distinct microbial pathways. Nature *509*, 361-365.

Dias, J., Boulouis, C., Gorin, J.B., van den Biggelaar, R., Lal, K.G., Gibbs, A., Loh, L., Gulam, M.Y., Sia, W.R., Bari, S., *et al.* (2018). The CD4(-)CD8(-) MAIT cell subpopulation is a functionally distinct subset developmentally related to the main CD8(+) MAIT cell pool. Proc. Natl. Acad. Sci. U.S.A. *115*, E11513-E11522.

Dias, J., Sandberg, J.K., and Leeansyah, E. (2017). Extensive Phenotypic Analysis, Transcription Factor Profiling, and Effector Cytokine Production of Human MAIT Cells by Flow Cytometry. Methods Mol. Biol. *1514*, 241-256.

Dias, J., Sobkowiak, M.J., Sandberg, J.K., and Leeansyah, E. (2016). Human MAIT-cell responses to Escherichia coli: activation, cytokine production, proliferation, and cytotoxicity. Journal of leukocyte biology *100*, 233-240.

Gamage, A.M., Zhu, F., Ahn, M., Foo, R.J.H., Hey, Y.Y., Low, D.H.W., Mendenhall, I.H., Dutertre, C.A., and Wang, L.F. (2020). Immunophenotyping monocytes, macrophages and granulocytes in the Pteropodid bat Eonycteris spelaea. Sci. Rep. *10*, 309.

Lim, T.P., Wang, R., Poh, G.Q., Koh, T.H., Tan, T.Y., Lee, W., Teo, J.Q., Cai, Y., Tan, T.T., Ee, P.L.R., *et al.* (2018). Integrated pharmacokinetic-pharmacodynamic modeling to evaluate empiric carbapenem therapy in bloodstream infections. Infect. Drug. Resist. *11*, 1591-1596.
Mak, J.Y., Xu, W., Reid, R.C., Corbett, A.J., Meehan, B.S., Wang, H., Chen, Z., Rossjohn, J., McCluskey, J., Liu, L., *et al.* (2017). Stabilizing short-lived Schiff base derivatives of 5-aminouracils that activate mucosal-associated invariant T cells. Nat. Commun. *8*, 14599.
Martinez Gomez, J.M., Periasamy, P., Dutertre, C.A., Irving, A.T., Ng, J.H., Crameri, G., Baker, M.L., Ginhoux, F., Wang, L.F., and Alonso, S. (2016). Phenotypic and functional characterization of the major lymphocyte populations in the fruit-eating bat Pteropus alecto. Sci. Rep. *6*, 37796.
Sia, W.R., Boulouis, C., Gulam, M.Y., Kwa, A.L., Sandberg, J.K., and Leeansyah, E. (2019). Quantification of human MAIT cell-mediated cellular cytotoxicity and antimicrobial activity. Methods Mol. Biol.
Sia, W.R., Boulouis, C., Gulam, M.Y., Kwa, A.L.H., Sandberg, J.K., and Leeansyah, E. (2020). Quantification of Human MAIT Cell-Mediated Cellular Cytotoxicity and Antimicrobial Activity. Methods Mol. Biol. *2098*, 149-165.